A SEARCH FOR CORONAL ACTIVITY AMONG TWO METAL-POOR SUBDWARFS AND ONE SUBGIANT

The Astronomical Journal, 152:43 (7pp), 2016 August doi:10.3847/0004-6256/152/2/43

A SEARCH FOR CORONAL ACTIVITY AMONG TWO METAL-POOR SUBDWARFS AND ONE SUBGIANT*

Graeme H. Smith[1], Andrea K. Dupree[2], and Hans Moritz Günther[3]
[1] University of California Observatories, Lick Observatory, Department of Astronomy & Astrophysics, UC Santa Cruz, 1156 High Street, Santa Cruz, CA 95064, USA; graeme@ucolick.org
[2] Harvard-Smithsonian Center for Astrophysics, Cambridge, MA 02138, USA; dupree@cfa.harvard.edu
[3] MIT Kavli Institute for Astrophysics and Space Research, Massachusetts Institute of Technology, Cambridge, MA 02139, USA; hgunther@mit.edu
Received 2016 April 7; revised 2016 May 25; accepted 2016 May 25; published 2016 August 4

ABSTRACT

A search has been made using the *XMM-Newton* satellite for coronal soft X-ray emission from HD 19445, HD 25329, and HD 140283, three Population II stars in the Galactic halo having metallicities of [Fe/H] ~ -2. The program stars, consisting of two subdwarfs and one metal-poor subgiant, were pre-selected from ground-based observations to have He I λ10830 absorption lines with an equivalent width (EW) of 30 mÅ or more. If such stars follow a relation between He I EW and soft X-ray flux applicable to Population I dwarf stars, then they would be expected to have X-ray luminosities $\sim 5 \times 10^{-7}$ times their bolometric luminosity, and as such would yield detectable sources in 20 ks exposures with the *XMM-Newton* EPIC-PN and MOS cameras. No detections were found in such exposures made with *XMM-Newton*. Upper limits to soft X-ray emission from the two program stars that have effective temperatures most similar to that of the Sun, namely HD 19445 and HD 140283, are comparable to the level of the quiet Sun. The star HD 25329, a cooler subdwarf, exhibits an upper limit similar to the Sun at maximum activity. These measurements suggest that coronal activity appears to decrease with age among the oldest G dwarfs, but K-M subdwarfs possibly have maintained a solar-like level of activity.

Key words: stars: coronae – stars: individual (HD 19445, HD 25329, HD 140283) – stars: Population II

1. INTRODUCTION

Coronal activity among main-sequence stars as measured by X-ray emission is known to be a decreasing function of age (e.g., Guedel et al. 1997; Feigelson et al. 2004; Preibisch & Feigelson 2005; Jackson et al. 2012). The limits of coronal activity are expected to be found among the metal-poor Population II subdwarf stars of the Galactic halo, which are among the oldest known stars in the Galaxy. Such subdwarfs do have chromospheres, as is evident from the spectroscopic detections of Ca II H and K emission and Mg II h and k emission lines among the closest of such stars (Peterson & Schrijver 1997; Smith & Churchill 1998; Isaacson & Fischer 2010). However, evidence for million degree coronae among metal-poor subdwarfs has been elusive to date. A technique often used for verifying the presence of a corona around a late-type dwarf star is the detection of soft X-ray emission. The *ROSAT* All Sky Survey detected few if any metal-poor stars of the Galactic halo with metallicities of [Fe/H] < -1.0 dex. In this paper we report a deep imaging search in soft X-rays made using the *XMM-Newton* spacecraft in an attempt to detect the presence of coronae around two Population II subdwarfs and one subgiant.

Within late-type dwarf stars coronal heating is thought to be governed by the activity of an interior magnetic dynamo, the strength of which depends on the stellar rotation rate. As stars evolve on the main sequence they spin down, with a consequent decrease in dynamo activity, coronal heating and consequently X-ray luminosity (e.g., Mamajek & Hillenbrand 2008; Wright et al. 2013). The dynamo spin-down model has met with success in describing the evolution of chromospheric and non-saturated (e.g., Pizzolato et al. 2003) coronal activity among main-sequence stars. However, the correlations between stellar activity and age, corner-stones on which the theory is based, depend largely on observations of stars younger than ~1 Gyr (Pizzolato et al. 2003; Wright et al. 2013). The evolution of coronal emission line fluxes among substantially older dwarfs remains poorly studied. With pre-selected stars chosen as described below, an *XMM-Newton* program has been carried out to search for soft X-ray emission from dwarf stars with metallicities (and therefore presumably ages) typical of the Galactic halo.

The program described in this paper was planned around a ground-based technique that can provide optimal Population II stars for deep soft-X-ray imaging. The He I triplet line at 10830 Å is known to serve as a tracer of chromospheric conditions among FGK stars (Zirin 1982; O'Brien & Lambert 1986; Zarro & Zirin 1986; Sanz-Forcada & Dupree 2008), and its behavior appears to be linked to the coronae of such stars. The process(es) responsible for populating the lower state of the 10830 Å triplet feature have been the subject of debate (e.g., Zirin 1976; Cuntz & Luttermoser 1990; Sanz-Forcada & Dupree 2008). Among Population I dwarfs later than spectral type F7 there is a correlation between soft X-ray flux and the equivalent width (EW) of the He I λ10830 line (Zarro & Zirin 1986; Takeda & Takada-Hidai 2011). This correlation has been documented down to X-ray flux levels corresponding to $\log(f_X/f_{bol}) \sim -6.3$ (Takeda & Takada-Hidai 2011). Furthermore, in the case of the Sun, spatial correlations exist between the λ10830 line strength and X-ray and EUV flux (e.g., Harvey & Sheeley 1977). As such the He I λ10830 line has been considered a proxy for coronal activity among main-sequence stars. The origin of the X-ray versus λ10830 absorption correlation is still debated, with one early interpretation being that it results from photoionization of He I by X-ray and EUV photons from the corona or transition region, followed by recombination to the triplet levels of neutral helium (e.g., Zirin 1975).

* Based on observations obtained with *XMM-Newton*, an ESA science mission with instruments and contributions directly funded by ESA Member States and NASA.

Table 1
Program Stars

Star HD	V[a] (mag)	$B-V$[a] (mag)	[Fe/H][a]	EW(λ10830)[b] (mÅ)	$\log(L_{bol}/L_{\odot})$[c]	L_{bol}[c] (10^{33} erg s^{-1})	T_{eff}[c] (K)	d (pc)
19445	8.06	0.45	−2.0	30	−0.06	3.34	6050	40
25329	8.49	0.87	−1.7	67	−0.79	0.62	4840	18
140283	7.21	0.49	−2.3	33	+0.63	16.34	5810	58

Notes.
[a] V, $B-V$, and [Fe/H] are from Gratton et al. (2000) for HD 19445 and HD 25329, and Norris et al. (1985) for HD 140283.
[b] Values for HD 19445 and HD 140283 from Takeda & Takada-Hidai (2011); for HD 25329 from Smith et al. (2012).
[c] For HD 19445 and HD 25329 the values of $\log(L_{bol}/L_{\odot})$ and T_{eff} are from Gratton et al. (2000). For HD 140283 they are based on T_{eff} and M_{bol} of Fuhrmann (1998).

In an effort to test for coronae among Population II subdwarfs, Smith et al. (2012) obtained spectra of the He I λ10830 line for more than 20 dwarfs with metallicity in the range $-2.1 \leqslant$ [Fe/H] $\leqslant -0.8$. Combined with the earlier work of Takeda & Takada-Hidai (2011), the observations show that metal-poor field subdwarfs commonly exhibit a λ10830 He I absorption feature. The equivalent width (EW) of the absorption is typically less than 70 mÅ among metal-poor subdwarfs, and for subdwarfs of $B-V$ color similar to the Sun the range is more normally from 0 to 40 mÅ. There is a greater range in λ10830 EW among Population I dwarfs, many of which have considerably stronger He I lines (EW >100 mÅ) than the subdwarfs. The EWs of Population I dwarfs do, however, overlap with the metal-poor subdwarfs despite the considerably greater age of the later (Smith et al. 2012). These results provide suggestive evidence that old subwarf stars may have coronae. Soft X-ray detections could verify this conclusion.

The most metal-poor halo subdwarfs are expected to be considerably older than the Population I dwarfs in the Zarro & Zirin (1986) survey. Yet as already noted, examples of metal-poor subdwarfs in Smith et al. (2012) have comparable He I EWs to some dwarfs in the Zarro & Zirin (1986) sample. The He I λ10830 lower level is evidently being excited among Population II subdwarfs. If radiative excitation from high-energy coronal photons is the relevant mechanism, then it would follow that subdwarfs should be detected in soft X-rays if sufficiently deep integrations can be acquired. None of the subdwarf stars in the He I study of Smith et al. (2012) are found as detections in the *ROSAT* All-Sky Survey Faint Source Catalog (Voges et al. 2000). This indicates a need for deeper pointed soft X-ray observations.

2. THE TARGET STARS

According to Takeda & Takada-Hidai (2011) the relation between EW(λ10830) and $\log(L_X/L_{bol})$ for dwarf stars with [Fe/H] > -1 extends down to EW(λ10830) = 33 mÅ at $\log(L_X/L_{bol}) = -6.2 \pm 0.3$. A number of subdwarfs are found in the Smith et al. (2012) and Takeda & Takada-Hidai (2011) observations with [Fe/H] < -1.0 and EW(λ10830) $\geqslant$ 30 mÅ. These represent an optimal pre-selected sample of stars with which to search for soft X-ray detections. We obtained deep *XMM-Newton* imaging with the EPIC camera system in an attempt to detect soft X-rays from two subdwarfs and one subgiant. The resulting observations constitute a feasibility study rather than a comprehensive search for soft X-ray emission along the subwarf main sequence. By chosing candidate stars according to He I λ10830 absorption lines we attempt to maximize the opportunity to detect soft X-ray emission.

Three stars were chosen for *XMM-Newton* deep imaging on the basis of several considerations: a He I λ10830 line with EW of 30 mÅ or greater, relatively bright apparent magnitudes of $V \sim$ 7–8, metallicity of [Fe/H] < -1.5 to ensure a true halo star, and an absence of bright nearby companions to minimize the risk of interloper sources. This led to the candidate stars that are listed in Table 1, which also contains values of photometric properties, metallicity, and the He I λ10830 EW. Optical images of the fields of the three stars show that there are no brighter stars within ∼15 arcmin of each of them. The sources of the V and $(B-V)$ photometry listed in Table 1 are Gratton et al. (2000) for HD 19445 and HD 25329 and Norris et al. (1985) for HD 140283, which are also the references for the tabulated [Fe/H] metallicity. Bolometric luminosities relative to solar are also listed for the stars in Table 1, together with effective temperatures. For both HD 19445 and HD 25329 the values of $\log(L_{bol}/L_{\odot})$ and T_{eff} are those derived by Gratton et al. (2000). In the case of HD 140283 the tabulated values are based on the effective temperature and bolometric magnitude obtained by Fuhrmann (1998). A bolometric luminosity for HD 140283 was also calculated from the effective temperature and gravity of Takeda & Takada-Hidai (2011), with an assumed stellar mass of $0.8M_{\odot}$, which gave $\log(L_{bol}/L_{\odot}) = 0.68$, in close agreement with the value of 0.63 from Fuhrmann (1998) listed in Table 1. Values of EW(λ10830) for HD 19445 and HD 140283 are from Takeda & Takada-Hidai (2011), while the analogous measurement for HD 25329 is from Smith et al. (2012).

The three stars in Table 1 have metallicities that are typical of the old Galactic halo. HD 140283 is the optically brightest star in the sample and has an effective temperature similar to the Sun. HD 19445 also has a solar-like effective temperature not much different from that of HD 140283. Both stars have bluer $(B-V)$ colors than the Sun due to their low metallicity. HD 25329 has the largest EW for the λ10830 He I line and so has considerable astrophysical interest, but it is cooler than the other two stars in Table 1, and so less comparable to well-studied solar-like dwarfs of the Galactic disk.

As can be seen from the luminosities and effective temperatures in Table 1, two of the program stars, HD 19445 and HD 25329, are subdwarf members of the metal-poor Galactic halo, and if they have ages similar to that of the globular cluster M92 they would be $\sim 12.5 \pm 0.5$ Gyr old (VandenBerg et al. 2014). HD 140283 is a metal-poor Galactic halo star with a relatively low metallicity of [Fe/H] ~ -2.3, and references to prior studies of it can be found in Bond et al. (2013) and VandenBerg et al. (2014). VandenBerg et al. (2014)

Table 2
XMM-Newton Observation Log

Star HD	ObsID	Observation Date	Exp Time (ks)	R.A. Epoch Obs.	decl. Epoch Obs.
19445	0741680201	2014 Aug 21T06:32:11	22	$03^h08^m25\overset{s}{.}4$	$+26°19'39\overset{''}{.}2$
25329	0741680301	2015 Mar 16T19:29:58	22	$04^h03^m12\overset{s}{.}7$	$+35°16'03\overset{''}{.}0$
140283	0741680101	2014 Aug 01T22:01:54	23	$15^h43^m02\overset{s}{.}0$	$-10°56'00\overset{''}{.}6$

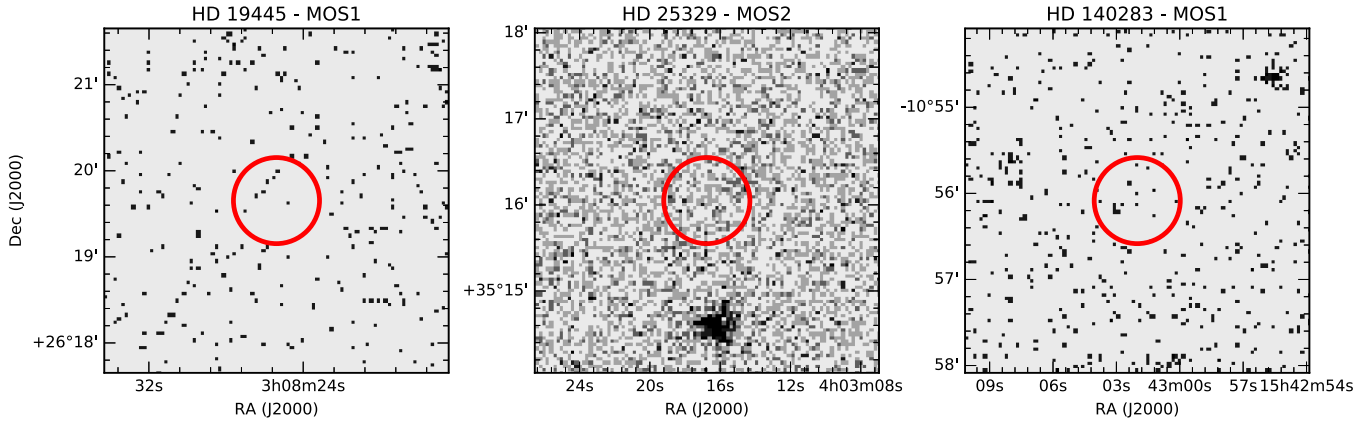

Figure 1. *XMM-Newton* 20 ks exposures of the three program stars. The red circle marks the count-extraction region at the position of each star. Left: MOS-1 image of the field of HD 19445. This subdwarf has an effective temperature and a bolometric luminosity similar to the Sun, but a much lower metallicity of [Fe/H] = −2.0. Center: MOS-2 image of the field of HD 25329. This metal-poor subdwarf is both cooler and less luminous than the Sun. Right: MOS-1 image of the field of HD 140283. This metal-poor subdwarf has an effective temperature similar to the Sun but a bolometric luminosity that is a factor of 4 times higher.

consider HD 140283 to be a subgiant, and a comparison of this star to isochrones in the ($\log T_{\rm eff}$, M_V) diagram lead them to derive an age of 14.3 ± 0.4 Gyr on the basis of a parallax measurement made with the Fine Guidance Sensor on the *Hubble Space Telescope*. For HD 140283 they find an absolute magnitude of $M_V = 3.37 \pm 0.03$, an effective temperature of 5797 K (which agrees well with the value listed in Table 1), and a *HST* FGS parallax of 17.2 ± 0.7 mas. The location of this star in the H-R diagram shown in Figures 1 and 2 of VandenBerg et al. (2014) places it part way between the main-sequence turn-off and the base of the red giant branch. As such, HD 140283 is in a more evolved state than the other two stars of our *XMM-Newton* program, and may be older than them by ∼ 1.5 Gyr (VandenBerg et al. 2014). The comparison between HD 19445 and HD 140283 is worth noting in that these two stars have very similar [Fe/H] metallicities, effective temperatures, and λ10830 He I EWs, while the later is in a more evolved state, although it has not yet arrived at the base of the red giant branch.

3. *XMM-NEWTON* OBSERVATIONS AND DATA REDUCTION

The *XMM-Newton* observations for this program (PI Smith) were obtained in 2014 August and 2015 March. The three targets HD 19445, HD 25329, and HD 140283 were observed with *XMM-Newton* for about 20 ks each. The *XMM-Newton* spacecraft operates several instruments in parallel; this program used the three X-ray imaging CCD cameras PN, MOS1, and MOS2, which comprise the European Photon Imaging Camera (EPIC; Strüder et al. 2001; Turner et al. 2001). A summary of the EPIC data, which were obtained in Full Frame mode for all three stars, is given in Table 2. The Medium filter was used for all observations in each camera.

The data reduction was carried out using the Science Analysis system (Gabriel et al. 2004) version 14.0.0. Standard filtering was applied to all event grades, but no filtering on high background intervals was done. The observation of HD 19445 has such low background rates that filtering is unnecessary. The same is true for the MOS detectors in the observation of HD 140283; in this observation the PN shows count rates around 13 counts s^{-1}, which is far above the recommended cut-off value, but inspection of the image shows that the background is concentrated on one specific chip edge of the PN. This chip is not relevant for the analysis, and the background on the remaining detector is below the value recommended for filtering. In the observation of HD 25329, the PN and both MOS detectors measured background rates roughly an order of magnitude above the limits used in standard filtering. The background is variable, but there is insufficient integration time at low backgrounds for any useful analysis. Thus, we include the full exposure time in the following and note that this leads to much looser upper limits compared to the other two observations.

The position of each star was calculated for the epoch of observation based on HIPPARCOS coordinates and proper motions (the resulting coordinates being listed in Table 2). A circular source extraction region with a radius of 30″ was placed on the calculated positions within each data frame. The background was estimated from regions on the same chip, by selecting circular regions with at least ten times the area of the source region, and taking care to avoid chip edges and sources in the field. In the case of the PN detectors, the background regions are placed at roughly the same distance from the read-out node, since this affects the electronic noise level. One exception is the observation of HD 19445, where both source and background region in the PN frame need to be smaller

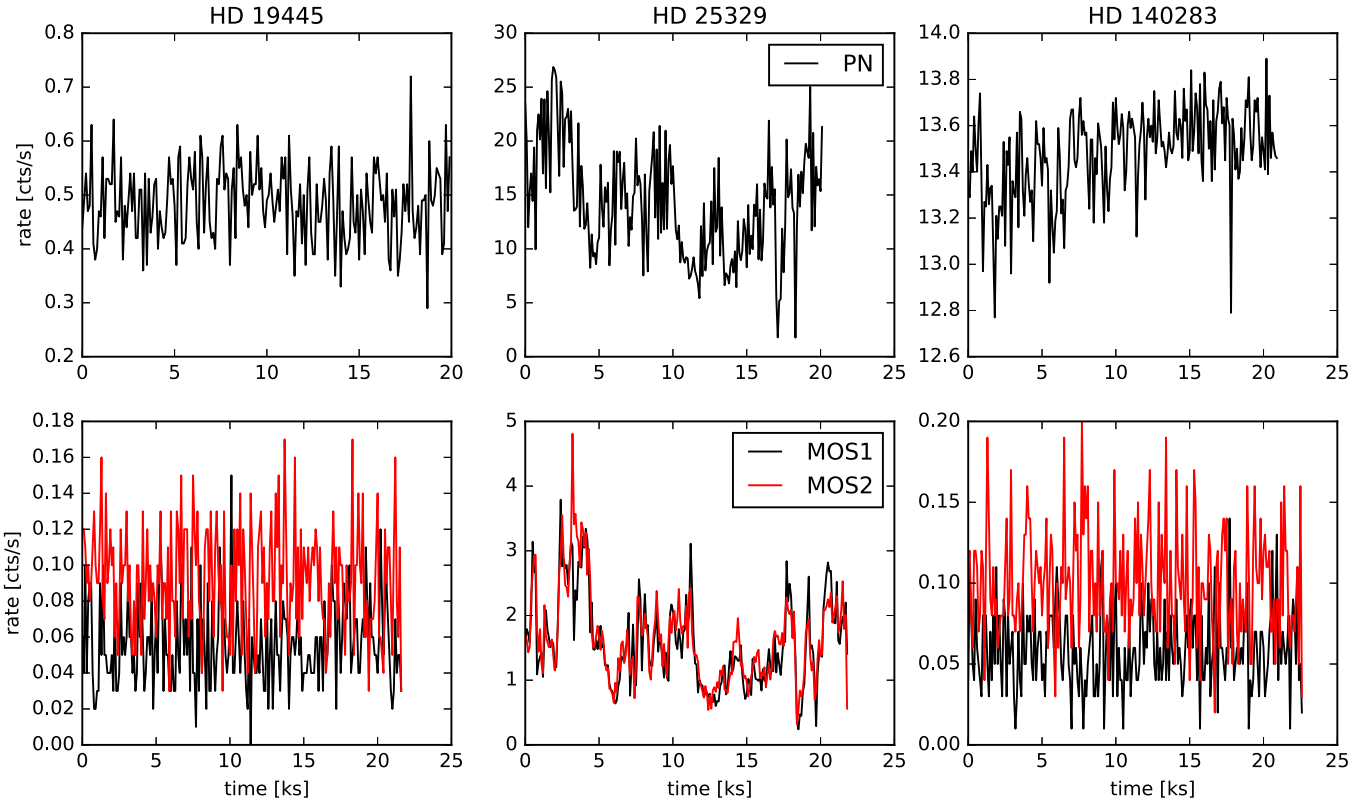

Figure 2. Full frame count rates in the EPIC PN, MOS1, and MOS2 chips vs. elapsed exposure time for the program stars HD 19445, HD 25329 and HD 140283. The PN full frames rates are shown in the top row of panels. Usually times with rates greater than 3.0 counts s^{-1} were filtered out. The lower row of panels plots the MOS1 and MOS2 rates as red and black lines. In the case of the HD 19445 and HD 140283 exposures with this pair of chips, times at which the count rate was greater than 0.4 counts s^{-1} were usually filtered out. The exposures of HD 25329 are characterized by high and time-variable background counts.

Table 3
Upper Limits on Stellar X-Ray Flux and Luminosity

Star HD	0.2–7 keV (counts s^{-1})	0.2–1.5 keV (counts s^{-1})	O VII (counts s^{-1})	f_X (0.2–5 keV) (10^{-15} erg cm^{-2} s^{-1})	L_X (0.2–5 keV) (10^{26} erg s^{-1})	$\log(L_X/L_{bol})$
19445	0.0007	0.0003	0.0001	<2	<4	<−6.9
25329	0.0025	0.0020	0.0009	<16	<6	<−6.0
140283	0.0005	0.0004	0.0002	<3	<11	<−7.2

(radius 20″) to avoid detector rows with high noise level at the chip edge.

Reproductions of the EPIC CCD images of all three fields are shown in Figure 1. None of the three program stars is detected in the observations. The full frame count rates for the EPIC PN, MOS1, and MOS2 chips are plotted versus elapsed exposure time for each program star in Figure 2. The variations are largely due to noise or background fluctuations, most notably in the case of the exposures of HD 25329 as noted above. Upper limits on the count rates from the stellar sources were calculated following the recipe employed for the *XMM-Newton Upper Limit Server*:[4] the background count rate was normalized to the same area used for the source extraction. Since it is measured from a much larger region, the uncertainty on the background count rate is small. A 95% confidence upper limit to each source flux was calculated following the Bayesian approach of Kraft et al. (1991) with a uniform prior. Considering the detectors separately, the MOS detectors always have more stringent limits than the PN, because of their lower background. Table 3 shows the strictest upper limit seen in the MOS1 or MOS2 chips for the three sources. Upper limits are calculated for three energy bands. A typical stellar corona emits predominantly at low energies, while at high energies the background emission dominates. Thus we select the following energy bands: 0.2–1.5 keV, 0.2–7.0 keV, and 0.465–0.665 keV. The last band is centered on the 0.57 keV O VII He-like triplet, which shows prominent emission for cool-star coronae (e.g., Ness et al. 2004). Reducing the background by filtering on this narrow energy band allowed Hempel et al. (2005) to detect β Pic in an *XMM-Newton* observation.

In order to convert the count rate limits in Table 3 to flux and luminosity limits it is necessary to assume a spectral model. The flux limits in the table are calculated for a corona with a solar abundance pattern with a 10^6 K temperature and no interstellar absorption using the WebPIMMS tool[5] and an APEC model (Foster et al. 2012).

These limits depend only weakly on the abundance (taking a global metallicity of 0.01 solar changes the average energy of

[4] http://www.cosmos.esa.int/web/xmm-newton/uls-userguide

[5] http://ledas-www.star.le.ac.uk/cgi-bin/w3pimms/pim

the X-ray photons by less than 1%) and the temperature (e.g., a coronal temperature of 3×10^6 K would lead to a flux limit 30% lower). The strictest limits can be derived using the count rate in the 0.2–1.5 keV band. Narrower bands have too few counts and thus larger Poisson fluctuations; wider bands include more background with (assuming a typical coronal spectrum) little additional source signal. Flux and luminosity limits in Table 3 are given in the 0.2–5.0 keV band for the stellar distances listed in Table 1. The corresponding upper limits to $\log(L_X/L_{bol})$ are also given in Table 3.

4. DISCUSSION

The results for each star can be summarized as follows. The subdwarf HD 19445 has an effective temperature and a bolometric luminosity similar to the Sun, but a much lower metallicity of [Fe/H] = −2.0. As such it provides the best analogy in our sample to a metal-poor counterpart to the Sun. Being a halo subdwarf, the age of HD 19445 is expected to be ∼12.5 Gyr if it is similar to that of the globular cluster M92 (VandenBerg et al. 2014). The upper limit placed on the soft X-ray luminosity of this subdwarf is 4×10^{26} erg s^{-1}, which corresponds to $\log L_X/L_{bol} = -6.9$. The X-ray luminosity of the Sun in the *ROSAT-PSPC* band ranges from 2×10^{26} erg s^{-1} at solar minimum to 2×10^{27} erg s^{-1} at solar maximum (Ayres 2014). Relative to the solar bolometric luminosity the solar X-ray luminosity ranges from $\log(L_X/L_\odot) = -7.28$ at solar minimum to −6.28 dex at solar maximum. The upper limit that the *XMM-Newton* observation imposes on the coronal activity of HD 19445 approaches the solar minimum level to about a factor of two.

The effective temperature of HD 140283 is also similar to that of the Sun but the bolometric luminosity is a factor of 4 times higher. The upper limit placed on the soft X-ray luminosity of HD 140283 is 11×10^{26} erg s^{-1}, which is the highest of the three stars in our sample and a factor of 6 times higher than that of the Sun at the minimum of its activity cycle. Nonetheless the upper limit on the ratio $\log L_X/L_{bol}$ of −7.2 is the lowest of the three stars observed. This relatively low upper limit on L_X/L_{bol} for HD 140283 is in part a reflection of the fact that this star has evolved from the Population II main sequence to a bolometric luminosity in excess of that of the Sun, as noted in Section 2. Wright (2004) found that Population I dwarfs with Maunder minimum type states of stellar activity have often notably evolved away from the zero-age main sequence, often by more than 1 mag in M_V. Perhaps HD 140283 is exhibiting a metal-poor equivalent of this phenomenon. The (M_V, $B-V$) H-R diagram shown in Figure 6 of Wright (2004) indicates that many Population I stars having chromospheric emission of $\log R'_{HK} < -5.1$ have evolved significantly away from the main sequence, possibly analogous to HD 140283.

An upper limit of 6×10^{26} erg s^{-1} is placed on L_X for the subwarf HD 25329. This is about three times the level of the Sun at minimum. However, because HD 25329 is both cooler and less luminous than the Sun, the corresponding upper limit on $\log L_X/L_{bol}$ is a relatively high value of −6.0, and comparable to that of the Sun at solar maximum. It is possible that this cooler subwarf HD 25329 could have a more active corona than the quiet Sun, but the high background counts encountered in the *XMM-Newton* exposures have prohibited a potential detection of possible coronal activity at this level.

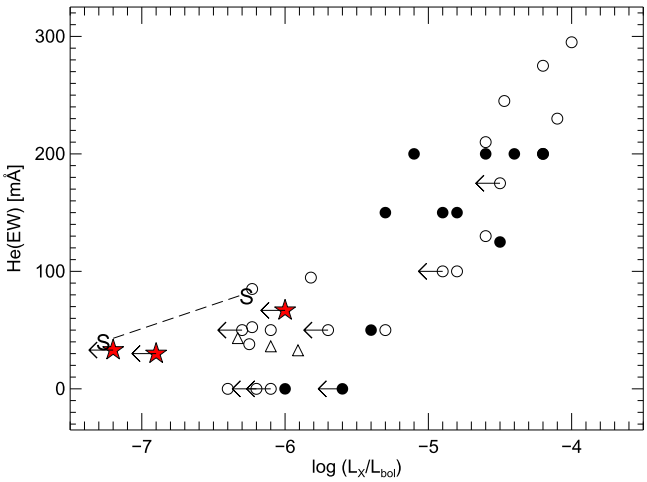

Figure 3. Equivalent width of the He I λ10830 feature vs. the ratio of soft X-ray luminosity to bolometric luminosity for dwarf stars in the studies of Zarro & Zirin (1986) and Takeda & Takada-Hidai (2011). Stellar spectral class is denoted: F7-G8 (open circles), K (filled circles). Stars with [Fe/H] < −0.4 are marked by open triangles. The metal-poor stars from the *XMM-Newton* program reported here are marked by a star symbol along with an arrow indicating an upper limit. The range of L_X/L_{bol} for the Sun in the *ROSAT*/PSPC band (Ayres 2014) is shown by the dashed line bounded by the letter S. The equivalent width at solar maximum and minimum is taken from the study of Livingston (1992), who finds a variation from ∼40 mÅ at solar minimum to ∼80 mÅ at solar maximum.

In terms of absolute X-ray luminosity the upper limits placed on all three program stars are within a factor of 6 of the solar X-ray luminosity at solar minimum. In the case of the near-solar-temperature stars HD 19445 and HD 140283 the ratio L_X/L_{bol} approaches, or is comparable to, the solar minimum value.

Further context for the present non-detections can be had by revisiting the correlation between soft X-ray luminosity and He I λ10830 EW for Population I dwarfs using published data. Zarro & Zirin (1986) used observations from the *Einstein* satellite to document a correlation between He I EW and the X-ray to bolometric luminosity ratio $\log L_X/L_{bol}$ for F-K dwarfs of spectral type F7 and later. To this work we added the data of Takeda & Takada-Hidai (2011) for a sample of low-activity dwarfs, their X-ray measurements being obtained from the *ROSAT* satellite. Four stars are in common between these two studies, and an unweighted average of the He I EW has been adopted here. The resulting plot of He I EW versus $\log L_X/L_{bol}$ is shown in Figure 3, and the spectral types of the stars plotted range from mid-F to K, so that they are not all dwarfs of solar-like effective temperatures.

The data on HD 25329 do not impose any new constraints on Figure 3 due to the relatively bright upper limit that was achieved for L_X/L_{bol}, which in turn was elevated by the high background counts of the CCD images for this star. If Figure 3 were to apply to the stars with EW(λ10830) = 30 mÅ observed in our *XMM-Newton* program one might have expected to detect soft X-ray emission within the range $-6.4 \leqslant \log(L_X/L_{bol}) \leqslant -5.2$. However, the upper limits on L_X/L_{bol} for both HD 19445 and HD 140283, two stars with near-solar effective temperatures, fall outside of this range, being lower by 0.5 dex or more. Both stars fall to the left of the distribution of dwarfs in Figure 3, and at a level comparable to the integrated quiet Sun flux.

The EW(λ10830) measurements less than 100 mÅ as given by Zarro & Zirin (1986) tend to be quantized as either 0 or 50 mÅ, except in one case where a value of 25 mÅ is given. The increments between the EW values presumably reflect the uncertainties in these measurements. As such, some stars for which Zarro & Zirin (1986) give an EW of 0 mÅ potentially have weak λ10830 lines with EWs of several tens of mÅ, which would mean a He I line of similar EW to HD 19445 and HD 140283, the two stars with solar-like effective temperatures in our program. The one star for which Zarro & Zirin (1986) give a λ10830 EW of 25 mÅ is HD 161797, a slightly metal-rich G5 IV star with an *Einstein* soft X-ray luminosity of $\log(L_X/L_{bol}) = -6.4$ and $T_{eff} = 5562$ K (Jofré et al. 2015). Both HD 19445 and HD 140283 have similar strengths of the λ10830 He I line but the *XMM-Newton* upper limits on $\log(L_X/L_{bol})$ are 0.5 dex or more below the *Einstein* measurement for HD 161797. The solar-like G0V star HD 19373 ($T_{eff} = 5648-5838$ K, Boyajian et al. 2013) and HD 121370 (G0 IV, $T_{eff} = 5967-6074$K, Boyajian et al. 2013) both have $\log(L_X/L_{bol}) = -6.4$ and EW(λ10830) = 0 mÅ from Zarro & Zirin (1986). These two stars and HD 161797, with solar-like effective temperatures, have the lowest X-ray/bolometric luminosities actually detected by *Einstein* in the Zarro & Zirin (1986) sample. As can be seen from Figure 3 there are several dwarfs in the L_X/L_{bol} range -6.0 dex to -6.4 dex that have detected He I absorption lines of ~25–50 mÅ. Such stars appear to have more active coronae than solar-temperature subdwarfs.

In summary, three points might be drawn from Figure 3 and the observational limits given in Table 3. (1) At low coronal activity levels there is possibly an intrinsic spread in L_X/L_{bol} for a given EW(λ10830). (2) Figure 3 does not appear to contain solar-like dwarfs having coronal activity comparable to the level of the quiet Sun near solar minimum. (3) The two solar-temperature stars in our program, HD 19445 and HD 140283, with EW(λ10830) ~ 30 mÅ, fall to the left side, i.e., lower coronal activity level, of the distribution of stars in Figure 3, and the limits placed on their X-ray luminosities are consistent with coronae that are as quiet as that of the solar minimum. In this context it is worth restating that HD 19445 and HD 140283 were pre-selected on the basis of having λ10830 He I absorption features with EWs of ~30 mÅ. The cooler subdwarf HD 25329 has even stronger λ10830 absorption. Thus our sample was deliberately biased so as to increase the likelihood of detecting soft X-ray emission, should the correlation between (L_X/L_{bol}) and EW(λ10830) for Population I dwarfs also apply to subdwarfs. The non-detection of both stars implies that the typical coronal activity level to be expected among solar-temperature main-sequence stars of the Galactic halo is less than that of a "mean" Sun, and possibly comparable to or even less than the Sun at solar minimum. Such an inference would be consistent with the old ages of subdwarfs and a continued but slow decrease in coronal activity with age among the oldest G dwarfs in the Galaxy. There may be intrinsic scatter in both EW(λ10830) and L_X/L_{bol} among the oldest G-type dwarfs of both the Galactic halo and the disk, that accompanies differences in age and metallicity.

Takeda & Takada-Hidai (2011) argued that the presence of He I λ10830 EWs of $10 <$ EW(λ10830) < 100 mÅ among subdwarfs is consistent with old dwarf stars attaining a base level of activity that is driven by some heating mechanism unrelated to a magnetic dynamo. Schmitt (1997), Bercik et al. (2005) and others have used X-ray data to argue for a base-level to coronal activity among late-type main-sequence stars, possibly related to acoustic heating or heating related to a non-rotating convective dynamo. If the proposition of Takeda & Takada-Hidai (2011) is correct then the data presented in this paper would be consistent with the further surmise that the base level of coronal activity among solar-temperature Population II subdwarfs is no greater than that of the solar minimum. Furthermore, should it prove from a larger sample of stars that the soft X-ray luminosities of halo subdwarfs with [Fe/H] < -1.0 are systematically lower, on average, than the mean for Population I dwarfs having comparable He I line EWs, then conditions in the region from which the λ10830 He line forms may be less metallicity or age dependent than the level of coronal activity. This poses the question: do metal-poor Population II F-G dwarfs have hot transition regions analogous to those of Population I dwarfs but less active coronal activity?

Models of the average quiet Sun (Avrett 1992) show that the He 10830 Å line arises from the same level in the chromosphere as the Mg II emission core, so that core emission can indicate the state of the atmosphere. The surface flux of the Mg II emission in metal-poor dwarfs, including two of our program stars, HD 19445 and HD 140283, is also generally less, by a factor of three to five, than the solar value (Peterson & Schrijver 1997). However, this ratio exceeds the depletion of [Fe/H] which is $\sim 10^{-2}$ solar. Peterson & Schrijver (1997) noted that in dwarf stars, the Mg II line strengths appear insensitive to metallicity. Such behavior of Mg II suggests that the chromospheres may be hotter and denser in metal-depleted dwarfs—which could follow if the energy input is similar between dwarf stars of greatly different metallicity. A metal-poor atmosphere does not allow as much cooling due to radiative losses so that the temperature would be greater. A higher temperature will cause increased ionization and electron density.

The coolest and least luminous star in our program is HD 25329. A Population I dwarf of similar effective temperature would have a spectral type of ~K3. An upper limit of $\log(L_X/L_{bol}) \sim -6.0$ for this subdwarf having a 67 mÅ λ10830 line could place it among the lower coronal-activity F7-G8 dwarfs plotted in Figure 3, but it may fall to the left of the K dwarfs. A solar-like level of coronal activity cannot be ruled out for HD 25329. However, the Ca K line strength of this star appears comparable to the lowest K-line fluxes of solar abundance dwarfs (Isaacson & Fischer 2010), which given the amount of 10830 Å absorption would appear also to suggest a warmer chromosphere. In this context it is worth noting that the metal-poor M1 V Kapteyn's star (GJ 191) has been detected in soft X-rays with a 0.3–2.5 keV luminosity of $L_X = (2.4–6.0) \times 10^{26}$ erg s^{-1} (Schmitt & Liefke 2004; Guinan et al. 2016), which is consistent with the upper limit placed on the more metal-poor HD 25329. Thus, although coronal activity among the oldest F-G subdwarfs may approach the very low levels of the quiet Sun, it is possible that among the K-M subdwarfs such activity is maintained.

Support for H.M.G. was provided by NASA through the Smithsonian Astrophysical Observatory (SAO) contract SV3-73016 to MIT for Support of the *Chandra* X-Ray Center (CXC) and Science Instruments. CXC is operated by SAO for

and on behalf of NASA under contract NAS8-03060. We thank the referee for helpful comments.

Facility: XMM-Newton.

REFERENCES

Avrett, E. H. 1992, in Proc. Workshop on the Solar Electromagnetic Radiation Study for Solar Cycle 22, ed. R. F. Donnelly (U.S. Dept. of Commerce), 20
Ayres, T. R. 2014, AJ, 147, 59
Bercik, D. J., Fisher, G. H., Johns-Krull, C. M., & Abbett, W. P. 2005, ApJ, 631, 529
Bond, H. E., Nelan, E. P., VandenBerg, D. A., Schaefer, G. H., & Harmer, D. 2013, ApJL, 765, L12
Boyajian, T. S., von Braun, K., van Belle, G., et al. 2013, ApJ, 771, 40
Cuntz, M., & Luttermoser, D. G. 1990, ApJL, 353, L39
Feigelson, E. D., Hornschemeier, A. E., Micela, G., et al. 2004, ApJ, 611, 1107
Foster, A. R., Ji, L., Smith, R. K., & Brickhouse, N. S. 2012, ApJ, 756, 128
Fuhrmann, K. 1998, A&A, 330, 626
Gabriel, C., Denby, M., Fyfe, D. J., et al. 2004, in ASP Conf. Ser. 314, Astronomical Data Analysis Software and Systems (ADASS) XIII, ed. F. Ochsenbein, M. G. Allen, & D. Egret (San Francisco, CA: ASP), 759
Gratton, R. G., Sneden, C., Carretta, E., & Bragaglia, A. 2000, A&A, 354, 169
Guedel, M., Guinan, E. F., & Skinner, S. L. 1997, ApJ, 483, 947
Guinan, E. F., Engle, S. G., & Durbin, A. 2016, arXiv:1602.01912
Harvey, J. W., & Sheeley, N. R. 1977, SoPh, 54, 343
Hempel, M., Robrade, J., Ness, J.-U., & Schmitt, J. H. M. M. 2005, A&A, 440, 727
Isaacson, H., & Fischer, D. 2010, ApJ, 725, 875
Jackson, A. P., Davis, T. A., & Wheatley, P. J. 2012, MNRAS, 422, 2024
Jofré, E., Petrucci, R., Saffe, C., et al. 2015, A&A, 574, A50
Kraft, R. P., Burrows, D. N., & Nousek, J. A. 1991, ApJ, 374, 344
Livingston, W. 1992, in Proc. Workshop on the Solar Electromagnetic Radiation Study for Solar Cycle 22, ed. R. F. Donnelly (U.S. Dept. of Commerce), 11
Mamajek, E. E., & Hillenbrand, L. A. 2008, ApJ, 687, 1264
Ness, J.-U., Güdel, M., Schmitt, J. H. M. M., Audard, M., & Telleschi, A. 2004, A&A, 427, 667
Norris, J., Bessell, M. S., & Pickles, A. J. 1985, ApJS, 58, 463
O'Brien, G. T., Jr., & Lambert, D. L. 1986, ApJS, 62, 899
Peterson, R. C., & Schrijver, C. J. 1997, ApJL, 480, L47
Pizzolato, N., Maggio, A., Micela, G., Sciortino, S., & Ventura, P. 2003, A&A, 397, 147
Preibisch, T., & Feigelson, E. D. 2005, ApJS, 160, 390
Sanz-Forcada, J., & Dupree, A. K. 2008, A&A, 488, 715
Schmitt, J. H. M. M. 1997, A&A, 318, 215
Schmitt, J. H. M. M., & Liefke, C. 2004, A&A, 417, 651
Smith, G. H., & Churchill, C. W. 1998, MNRAS, 297, 388
Smith, G. H., Dupree, A. K., & Strader, J. 2012, PASP, 124, 1252
Strüder, L., Briel, U., Dennerl, K., et al. 2001, A&A, 365, L18
Takeda, Y., & Takada-Hidai, M. 2011, PASJ, 63, 547
Turner, M. J. L., Abbey, A., Arnaud, M., et al. 2001, A&A, 365, L27
VandenBerg, D. A., Bond, H. E., Nelan, E. P., et al. 2014, ApJ, 792, 110
Voges, W., Aschenbach, B., Boller, Th., et al. 2000, VizieR on-Line Data Catalog: IX/29
Wright, J. T. 2004, AJ, 128, 1273
Wright, N. J., Drake, J. J., Mamajek, E. E., & Henry, G. W. 2013, AN, 334, 151
Zarro, D. M., & Zirin, H. 1986, ApJ, 304, 365
Zirin, H. 1975, ApJL, 199, L63
Zirin, H. 1976, ApJ, 208, 414
Zirin, H. 1982, ApJ, 260, 655